

BTO 2018.015 | April 2018

## **BTO** report

Closing the gap between  
small and smaller:  
Towards a framework to  
analyse nano- and  
microplastics in aqueous  
environmental samples



# BTO

## Closing the gap between small and smaller: Towards a framework to analyse nano- and microplastics in aqueous environmental samples

BTO 2018.015 | April 2018

### Project number

402045-053

### Project manager

Stefan Kools

### Client

BTO - Thematical research - New monitoring concepts

### Quality Assurance

Annemarie v. Wezel

### Author(s)

S.M. Mintenig, P.S. Bäuerlein, A.A. Koelmans, S.C.  
Dekker, A.P. van Wezel

### Sent to

This report is distributed to BTO-participants and is  
public.

**Year of publishing**  
2018

**More information**  
Patrick Bauerlein  
T 702  
E [patrick.bauerlein@kwrwater.nl](mailto:patrick.bauerlein@kwrwater.nl)

**Keywords**

Postbus 1072  
3430 BB Nieuwegein  
The Netherlands

T +31 (0)30 60 69 511  
F +31 (0)30 60 61 165  
E [info@kwrwater.nl](mailto:info@kwrwater.nl)  
I [www.kwrwater.nl](http://www.kwrwater.nl)

**KWR** Watercycle  
Research  
Institute

BTO 2018.015 | April 2018 © KWR

All rights reserved.

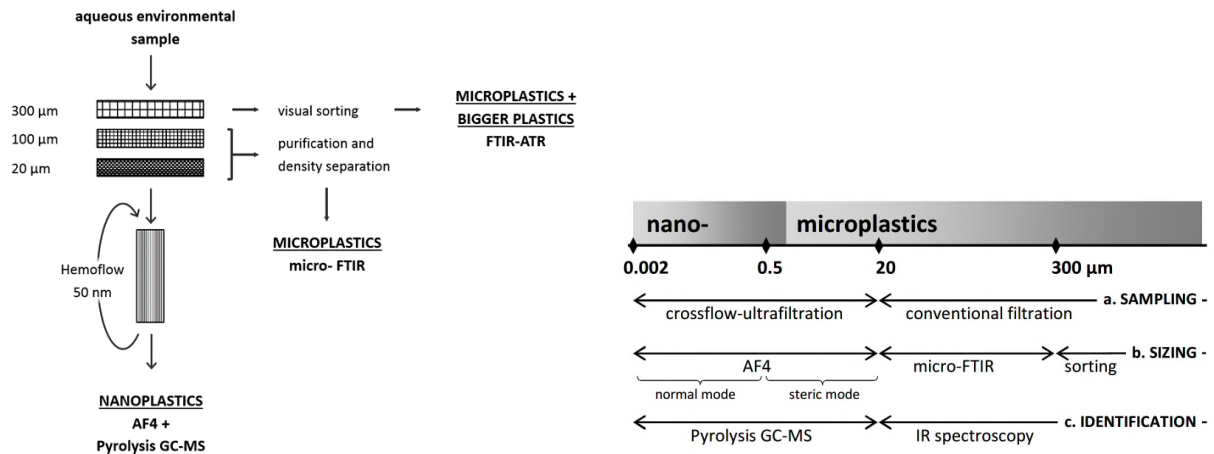
No part of this publication may be reproduced, stored in an automatic database, or transmitted, in any form or by any means, be it electronic, mechanical, by photocopying, recording, or in any other manner, without the prior written permission of the publisher.

## BTO Managementsamenvatting

### Micro- en nanoplastics: op weg naar het meten van steeds kleinere plasticdeeltjes

**Auteur(s)** Svenja Mintenig, dr. Patrick Bäuerlein, prof.dr. Bart Koelmans, prof.dr. Stefan Dekker, prof.dr. Annemarie van Wezel

In een eerste stap om de mate van vervuiling van Nederlandse binnenwateren met nanoplastics in kaart te brengen, stelt dit onderzoek een meetstrategie en -methode voor om extreem kleine plasticdeeltjes te kunnen meten. Micro- en nanoplastics die als gevolg van plasticvervuiling in zee terechtkomen zijn schadelijk voor het zeeleven. In hoeverre nanoplastics ook in zoetwater voorkomen, is nog onduidelijk. Gezien de mogelijke gezondheidsrisico's van is kennisontwikkeling over plasticvervuiling belangrijk. Hoewel microplastics steeds beter meetbaar zijn ontbreekt een consistent meetprotocol waarmee ook de kleinere nanoplastics kunnen worden gemeten. Het hier gepresenteerde onderzoek wil hierin verandering brengen.



Overzicht van de toegepaste technieken voor de verschillende deeltjesgroottes: LOD (limit of detection), AF4-MALS (asymmetrical flow field flow fractionation - multi angle light scattering) en FTIR (fourier transformation - infrared spectroscopy) (rechts) en monsternameschema (links).

#### Belang: duidelijkheid nodig over plasticvervuiling

Al gedurende zo'n twee decennia raken allerlei wateren, met name oceanen, vervuild met plastic. Wetenschappelijk onderzoek maakt de gevolgen voor het zeeleven duidelijk zichtbaar. Dieren raken verstrikt in plastic netten en draden, of raken ondervoed omdat ze vooral plastic binnenkrijgen in plaats van voedsel.

Het voorkomen en de gevolgen van plastic nanodeeltjes, die te klein zijn om met een standaard microscoop waar te nemen, zijn echter grotendeels onbekend. De deeltjes ontstaan wanneer plastic in het milieu langzaam maar zeker uiteenvalt tot steeds kleinere stukjes. Er bestaat grote behoefte de aanwezigheid van nanoplastics in het aquatische

milieu kwantitatief en kwalitatief te kunnen aantonen en daarmee de mate van plasticvervuiling in kaart te

#### Aanpak: ontwikkelen meetprotocol en –methode

In de eerste stap van dit onderzoek is een protocol ontwikkeld voor het nemen van betrouwbare water monsters. Verschillende groottefracties van het monsters worden verzameld en elke fractie wordt afzonderlijk onderzocht. Met een concentratiestap via crossflow ultrafiltratie (Hemoflow) wordt de fractie met deeltjes rond de 50 nm geconcentreerd. Zowel de grootte, hoeveelheid als het polymeertype van de plastic deeltjes van elke fractie worden bepaald.

#### Resultaten: geslaagde metingen micro- en nanodeeltjes met verschillende technieken

Verschillende technieken zijn toepast voor het meten van de deeltjes. Asymmetrical field flow fractionation werd gebruikt om de grootte van nanodeeltjes te achterhalen en pyrolysis-GC/MS voor bepaling van het type plastic. Met micro-FIT-IR kunnen de grootte en het type plastic van deeltjes groter dan 28 µm worden bepaald. In combinatie met een crossflow ultrafiltratieopstelling was het mogelijk om de concentratie van deeltjes in een watermonster 200 keer te verhogen. Daarmee is een limit of detection voor nanoplastic van 20 µg/L haalbaar. Dit is belangrijk omdat plasticconcentratie van circa 100 µg/L al eerder zijn aangetoond in rwzi's

#### Implementatie: meetcampagne Dommel en Maas

Om werkbaarheid ervan in de praktijk te testen wordt het ontwikkelde monsternameprotocol toegepast in een meetcampagne. Verder zal dit protocol worden aangevuld met een handleiding hoe monsters moeten worden opgewerkt. De monstername vindt plaats op verschillende locaties langs de Dommel en de Maas (inclusief rwzi's) en in drinkwaterbekkens. De data die uit dit onderzoek voortkomen zijn vervolgens bruikbaar voor modellering van plastic verspreiding in het Nederlandse milieu. Daarnaast krijgen waterbedrijven informatie over de aanwezigheid van micro- en nanodeeltjes in drinkwaterbronnen.

#### Rapport

Dit onderzoek is tot stand gekomen in het kader van het TRAMP project vanuit de NWO Toegepaste en Technische Wetenschappen (project number 13940), in samenwerking met het BTO, en beschreven in rapport *Closing the gap between small and smaller: Towards a framework to analyse nano- and microplastics in aqueous environmental samples* (BTO 2018.015) en in een wetenschappelijk artikel met dezelfde titel.

Year of publishing  
2018

More information  
Patrick Bauerlein  
T 702  
E patrick.bauerlein@kwrwater.nl

Keywords

Postbus 1072  
3430 BB Nieuwegein  
The Netherlands

T +31 (0)30 60 69 511  
F +31 (0)30 60 61 165  
E [info@kwrwater.nl](mailto:info@kwrwater.nl)  
I [www.kwrwater.nl](http://www.kwrwater.nl)

**KWR** Watercycle  
Research  
Institute

BTO 2018.015 | April 2018 © KWR

All rights reserved.

No part of this publication may be reproduced, stored in an automatic database, or transmitted, in any form or by any means, be it electronic, mechanical, by photocopying, recording, or in any other manner, without the prior written permission of the publisher.



## Closing the gap between small and smaller: Towards a framework to analyse nano- and microplastics in aqueous environmental samples

Received 00th January 20xx,  
Accepted 00th January 20xx

DOI: 10.1039/x0xx00000x

[www.rsc.org/](http://www.rsc.org/)

S.M. Mintenig<sup>a,b</sup>, P.S. Bäuerlein<sup>b</sup>, A.A. Koelmans<sup>c,d</sup>, S.C. Dekker<sup>a,e</sup>, A.P. van Wezel<sup>a,b</sup>

Detecting nanoplastics and determining actual concentrations and sizes of plastics present in the environment are essential to assess the hazards plastic particles pose. Microplastics have been detected globally in various aqueous ecosystems, but the determination of nanoplastics is lagging behind due to methodological challenges. Here, we propose a framework that is able to consistently determine a broad size spectrum of plastic particles in an aqueous environmental sample, and provide analytical results as proof of principle. Within the framework, microplastics are detected using FTIR microscopy. Nanoplastics are studied using field-flow-fractionation to obtain information on the particle sizes, and pyrolysis GC-MS is used to identify polymer types. Pyrolysis GC-MS seems promising for detecting nanoplastics in an environmental sample because to identify polystyrene (PS) a mass of approximately 100 ng is required. Pre-concentrating nanoplastics by crossflow ultrafiltration reduces the detection limits, enabling polystyrene to be identified when the original concentration in an aqueous sample is  $> 20 \mu\text{g L}^{-1}$ . Finally, we present an approach for estimating polymer masses based on the two-dimensional microplastic shapes recorded during the analysis with FTIR microscopy. Our suite of techniques demonstrates that analysis of the entire size spectrum of plastic debris is feasible.

**Keywords:** pollution, nanoplastic, monitoring, sampling, crossflow ultrafiltration

### 1. Introduction

A growing body of literature is documenting the widespread occurrence of plastic litter in various ecosystems<sup>1-3</sup> and its ecological consequences.<sup>4, 5</sup> Considerable attention has been given to microplastics (MP): plastics smaller than 5 mm.<sup>6, 7</sup> MP and smaller particles known as nanoplastics (NP) can be released to the environment directly<sup>8, 9</sup> or can be formed when larger plastic items degrade and fragment under the impact of various environmental stressors.<sup>10-12</sup> The actual fragmentation processes are unknown and currently under research.<sup>13, 14</sup> However, it is widely assumed that the fragmentation into small MP and eventually into NP is one of the explanations for the “missing plastic” budget, a term defined by Cozar *et al.*<sup>3</sup>, who detected lower MP concentrations in the open ocean surfaces than predicted by their model. Recent experimental, modelling and field studies further support this hypothesis.<sup>11-13, 15, 16</sup>

MP has been studied and detected globally in almost all natural habitats, but no lower size limitations or sub-classes have been officially defined. This implies that nano-sized plastics are also defined as MP. Yet the term “nanoplastic” is widely used, but interpreted differently. Some authors follow the EU definition of nanomaterials (2011/696/EU)<sup>8, 17</sup>, according to which, at least 50% of the particles must have at least one dimension smaller than 100 nm; other studies define NP as plastic particles  $< 1 \mu\text{m}$ <sup>11, 16, 18</sup> or even  $< 20 \mu\text{m}$ .<sup>19</sup> Here, we adopt a size limit of  $< 1 \mu\text{m}$ , as this is the limit used in most of the recent literature on MP and NP.

There are currently several protocols for detecting MP<sup>20</sup>, but they lack consistency in sampling, sample pre-treatment, analysing and reporting of results. The analysis of NP is more elaborate, and protocols are currently under development.<sup>16</sup> One of the major challenges is the pre-concentration of samples required to match the detection limits of currently available instrumentation. The aim of the present paper is twofold. First, we aim to provide a framework for quantitatively analysing NP and MP that is based on three criteria: (a) a sampling strategy to reproducibly concentrate plastic particles of targeted sizes, (b) the determination of particle sizes and (c) the identification of polymer types. Second, we aim to provide empirical data on the applicability of novel steps in the proposed framework.

<sup>a</sup> Copernicus Institute of Sustainable Development, Utrecht University, The Netherlands.

<sup>b</sup> KWR Watercycle Research Institute, Nieuwegein, The Netherlands.

<sup>c</sup> Aquatic Ecology and Water Quality Management Group, Wageningen University, The Netherlands.

<sup>d</sup> Wageningen Marine Research, IJmuiden, The Netherlands.

<sup>e</sup> Faculty of Management, Science and Technology, Open University, Heerlen, The Netherlands

Electronic Supplementary Information (ESI) available: See DOI: 10.1039/x0xx00000x

## 2. A framework for the analysis of nano- and microplastics in aqueous environmental samples

In order to concentrate MP and NP for a representative analysis, starting with an appropriate sampling strategy is of high importance. The protocol used most widely today entails filtering surface water through nets with a mesh size of 333  $\mu\text{m}$ .<sup>1, 2, 21, 22</sup> The size of smaller particles retained is 25 to 45  $\mu\text{m}$  when water is filtered through a stack of sieves<sup>23, 24</sup>, and 10  $\mu\text{m}$  when stainless steel cartridge filters are used.<sup>25</sup> Sampling NP is more challenging as conventional filtering is not applicable in these low size ranges. Ter Halle, *et al.*<sup>16</sup> used ultrafiltration to concentrate the colloidal fraction (< 1.2  $\mu\text{m}$ ) of a 1 L seawater sample. Another concentration technique is crossflow ultrafiltration, which uses a filter originally made as dialysis equipment (Hemoflow, Fresenius Medical Care, Germany). This crossflow ultrafiltration setup has been applied successfully to concentrate microorganisms in drinking and surface waters by factors of 4000 and 1000, respectively.<sup>26</sup>

To date, a variety of analytical techniques has been applied to determine MP in environmental samples. Numerous studies have relied on visual sorting of MP of a few hundred  $\mu\text{m}$  micrometres in size.<sup>1, 27</sup> In recent years, the scientific focus has shifted from determining visible plastic particles to determining microscopic plastic particles, usually using spectroscopic<sup>28-30</sup> or thermal degradation analyses.<sup>31-33</sup> When coupled to a microscope, Fourier transform infrared (FTIR) or Raman spectroscopy reveals the chemical identity of particles and allows the estimation of individual particle sizes and shapes. However, both techniques are limited by particle size: 500 nm for Raman microscopy<sup>29</sup> and 20  $\mu\text{m}$  for FTIR microscopy.<sup>28</sup> In contrast, thermal degradation analyses are not limited by size when analysing mixed environmental samples, but also, they do not provide information on particle sizes. Recent studies have used thermal degradation to identify polymer mixtures in surface water<sup>16</sup>, soil<sup>31, 34</sup>, fish<sup>33</sup> and wastewater treatment plant effluents.<sup>32</sup>

A major problem arising from using such different techniques is the incomparability of data.<sup>20, 35-37</sup> Manual particle sorting or spectroscopic analyses yield numbers of MP particles or fibres, whereas water volumes<sup>23, 38</sup>, surface areas<sup>2, 39</sup>, sediment weight<sup>40, 41</sup> and suspended particulate matter weight<sup>42</sup> are presented in metric units. A bigger problem occurs when comparing these data with data from thermal degradation procedures that aim to simultaneously identify and quantify polymers<sup>31, 33</sup> per sample volume or weight. Eventually, exposure data are needed that can be linked to results generated during effect studies. And as the hazards posed by MP and NP are likely to depend on the concentration, size<sup>5, 43</sup> and potentially on polymer types, these data are of high interest.<sup>44, 45</sup> Information on polymer masses will be required to enable mass-balance models that link production and emission data to environmental occurrence data.<sup>46, 15</sup>

Given that plastic debris comes in a broad spectrum of sizes, its identification requires a combination of different sampling techniques (criterion a) and analytical techniques to determine sizes (criterion b) and polymer types (criterion c) (Figure 1). The

sequence of the techniques, and their relationships, are shown also in a flow scheme (Figure S1). In addition to conventional filtration to concentrate MP, we introduce crossflow ultrafiltration to concentrate NP prior to analysis. For NP analysis two techniques are needed: Asymmetrical Flow Field-Flow Fractionation (AF4), which is a versatile tool for sample fractionation based on particle sizes<sup>47</sup>, in combination with pyrolysis gas chromatography–mass spectrometry (GC-MS), to identify polymers in size fractions collected individually. Here, a filtration step is essential since the particle size separation of the AF4 occurs in two modes: in the ‘normal’ mode, increasing particle sizes lead to an increased retention, whereas this is reversed for bigger particles in the so-called ‘steric’ mode. The sizes and polymer types of MP particles exceeding 20  $\mu\text{m}$  are identified with micro-FTIR (Figure 1). Manual sorting and subsequent identification of MP becomes feasible for plastics bigger than 300  $\mu\text{m}$ ; thus this common procedure<sup>1, 2, 20</sup> completes the proposed protocol.

The framework has several components new to this field of research that we have tested individually and in combination. These tests are presented below and comprised (a) sampling surface and drinking water by concentrating them using crossflow ultrafiltration, including the determination of recovery rates, (b) NP size determination using AF4 and (c) polymer identification of NP using pyrolysis GC-MS.

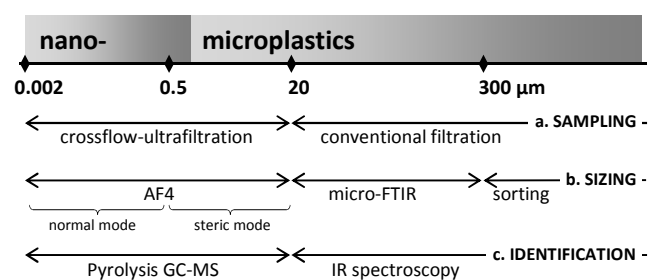


Figure 1: Protocol applied to: (a) sample; and detect sizes (b) and identify polymer types (c) of NP and MP in an environmental aqueous sample.

## 3. Materials and Methods

### 3.1 Materials and instrumental setup

**Chemicals** Monodispersed NP suspensions of polystyrene (PS) spheres with specified diameters (50, 100, 200, 500 and 1000 nm) and uncharged surfaces were purchased from Polyscience Inc. (Illinois, USA). Monodispersed nanoparticles (50 nm) made from gold and silver were purchased from NanoComposix (California, USA). Green fluorescent MP polyethylene (PE) beads in sizes ranging from 90 to 106  $\mu\text{m}$  were purchased from Cospheric (California, USA). To facilitate dosing, these PE beads were suspended in ultrapure water containing a surfactant (0.01% sodium dodecyl sulphate (SDS), Sigma Aldrich), which yielded a final concentration of 260 mg ( $5 \times 10^5$  particles)  $\text{L}^{-1}$ . To determine MP, the solutions were filtered through cellulose nitrate filters (0.45  $\mu\text{m}$  Whatman, Germany) and PE beads were counted using a dissecting microscope (Zeiss STEMISV8, Germany). Further, transparent PS pellets were cooled with

liquid nitrogen, ground and sieved over an installed 100  $\mu\text{m}$  mesh (Retsch Centrifugal Grinding Mill ZM1000, Germany).

**Crossflow ultrafiltration** To increase MP and NP concentrations we used a crossflow ultrafilter (Hemoflow filter HF80S, Fresenius, Medical Care) consisting of bundled hollow fibre membranes made of polysulfone that had an inner diameter of approximately 200  $\mu\text{m}$ . The exact pore sizes were not specified, but the cut-off was defined for proteins sized between 40 and 60 kDa. Samples were pumped (Masterflex, Cole Parmer, USA) through the crossflow ultrafilter at a constant flow rate of 4 L  $\text{min}^{-1}$  and an overpressure of 0.4 bar. Thereby the permeate was pressed through the filter while the concentrate was retained and rinsed back into the tank, raising particle concentrations (see Figure S2).

**AF4** An AF4 system was used (Postnova Analytics GmbH, AF2000, Landsberg, Germany), coupled online to a UV detector (Shimadzu) and a multi-angle light-scattering (MALS) detector (Postnova, Landsberg, Germany). The trapezoidal channel was 27.5 cm long and 250  $\mu\text{m}$  thick. There were two membranes, 10 kDa regenerated cellulose (RC) and 10 kDa polyethersulfone (PES) (Postnova, Landsberg, Germany), and three carrier liquids: ultrapure water ( $> 18 \text{ M}\Omega$ ), a solution containing an anionic surfactant (0.01% SDS, Sigma Aldrich) and a solution containing a non-ionic surfactant (0.01% TWEEN, Sigma Aldrich) surfactant. See Table S1. The fractionation and presence of particles were recorded by the MALS detector. Plotting the detection signal against the fractionation time, the area under the curve (AUC), proportional to the particle concentrations injected, was determined using GraphPad Prism (5.01, GraphPad Software, San Diego California USA). Further information on the general ability and limitations of the AF4 to separate particles can be found elsewhere.<sup>48, 49</sup>

**Pyrolysis GC-MS** Polymers in environmental samples were analysed using pyrolysis GC-MS. The samples were pyrolysed at 560  $^{\circ}\text{C}$  (Pyromat, GSG Mess- und Analysegeräte, Germany) in a tubular pyrolysis wire with a capacity of approximately 15  $\mu\text{L}$ . The instrumental details for pyrolysing a sample are provided as Supporting Information (Table S2). The degradation gases were separated using a GC (Trace GC, ThermoFisher Scientific, Madison, USA) and identified using an MS system (Trace MS Plus, ThermoFisher Scientific, Madison, USA). The settings of the GC-MS system are shown in Table S3. Generated pyrograms, peak intensities and polymer characteristic mass-to-charge ( $m/z$ ) ratios were analysed using the software XCalibur (Thermo XCalibur 2.2 SP1.48, ThermoFisher Scientific, Madison, USA). Individual compounds were searched within a library of organic compounds (NIST/EPA/NIH MS Library (NIST 11), USA) and an in-house polymer library.

**Micro-FTIR** An FTIR microscope equipped with an ultra-fast motorized stage and a single mercury cadmium telluride (MCT) detector (Nicolet iN10, ThermoFisher Scientific, Madison, USA) was used to identify MP, using chemical mapping. This entailed enrichment of the samples on aluminium oxide filters (Anodisc 25 mm, Whatman, UK) placed on a calcium fluoride ( $\text{CaF}_2$ ) crystal (EdmundOptics, Germany) to prevent filter bending. All measurements were taken in transmission mode (Löder, *et al.*<sup>28</sup>). Polymers were identified with the aid of the “Hummel

Polymer and Additives FTIR Spectral Library” (ThermoFisher Scientific, Madison, USA). The spectra and chemical maps generated were analysed using Picta software (1.5.120, ThermoFisher Scientific, Madison, USA).

**Samples** To test the individual techniques that make up the framework, samples of drinking and surface water were spiked with different monodispersed plastic particles. The drinking water was tapwater from Nieuwegein; the ultrapure water was obtained by purifying demineralized water in a Milli-Q system (Millipore, MA, USA). The surface water samples were from two freshwater systems in the Netherlands: the Lek canal and Lake IJssel. The Lek canal was sampled in April 2016 using a stainless steel bucket. Surface water of Lake IJssel was sampled using crossflow ultrafiltration (Figure S2) in January 2016. Using a water standpipe at an official sampling point, we obtained surface water pumped from a depth of 0.5 m by placing a small stainless steel cask with a volume of approximately 20 L under the open tap and allowing it to fill with water. The volume of water was maintained at a constant level by means of a float valve that allowed more water to be pumped into the cask automatically when the level fell. This allowed the concentration process to proceed unsupervised for 24 h. During this time, 635 L surface water were filtered and concentrated into a volume of 0.4 L. Contamination with plastic particles was minimized by using tubes rinsed with ultrapure water and by covering the tank with aluminium foil. Subsequently, the Lake IJssel sample was filtered through a 20  $\mu\text{m}$  stainless steel sieve, the retentate was treated with 1 M sodium hydroxide (NaOH, 3 days, 50  $^{\circ}\text{C}$ , similar to Dehaut, *et al.*<sup>50</sup>) and tested for MP. To do so, the sample was spread out evenly on a glass fibre filter for the pyrolysis GC-MS analysis and on an Anodisc filter for micro-FTIR analysis.

### 3.2 Testing the analytical framework using spiked and real environmental samples

**A) Sampling** Crossflow ultrafiltration was further evaluated by adding NP (PS 50 and 200 nm) or MP (PE 90-120  $\mu\text{m}$ ) to drinking water samples. For both plastic types, three 100 L samples were concentrated into final volumes of 0.5 L. Further, one sample of pure drinking water was filtered and used as a blank. For MP, the starting concentration was 2.6  $\mu\text{g}$  (5 particles)  $\text{L}^{-1}$ . For NP, 0.4  $\text{mg L}^{-1}$  PS (50 nm) and 0.585  $\text{mg L}^{-1}$  (200 nm) PS were added. Standard suspensions with particle concentrations 200 times higher than that were produced and used to determine NP recovery rates. Pre-concentration was done as follows. The 100 L were distributed among five jerry cans (20 L, HDPE) and pumped through the crossflow ultrafilter. Each jerry can was thoroughly rinsed with ultrapure water and ethanol (30%). After two hours the concentrate was collected in a glass jar, and the tubes and filters were rinsed twice by pumping 150 mL of collected permeate through the filter. The MP beads were counted using a dissecting microscope and the totals compared to the originally admixed concentrations. The NP samples and standard suspension were analysed in quadruplicate using AF4-MALS, and the AUCs were determined. The AUC was proportional for an NP concentration range of 0.1 to 140  $\text{mg L}^{-1}$

( $R^2 > 0.99$ ) and so was used to evaluate the NP recovery. In addition to AF4-MALS measurements, all NP samples were re-analysed using spectrophotometry (UNICAM UV 500, ThermoSpectronic). The UV absorbance was measured at 229 nm wavelength, at which PS in ultrapure water shows the highest absorption. The system was calibrated for PS concentrations between 4 to 23.6 mg L<sup>-1</sup>, resulting in a proportional absorbance ( $R^2 > 0.99$ ). The UV absorbance of the concentrated crossflow samples was measured after samples had been diluted with ultrapure water (1:10) and ultrasonicated for five minutes to prevent erroneous measurements arising from aggregation.

**B) Size determination** To detect the sizes of plastics accurately, different techniques were used. For MP, the two-dimensional shape (maximum and minimum diameters) of individual particles can be assessed during chemical mapping by using micro-FTIR, as will be explained in the following section. More challenging is the size determination for NP: although AF4 is a powerful technique for separating a variety of nanoparticles, it needs to be adapted for the particles of interest.<sup>47</sup> First, two membranes, RC and PES, were tested in combination with different carrier liquids: ultrapure water, or a solution containing an anionic (SDS) or a non-ionic (TWEEN) surfactant. These surfactants were added to reduce particle–membrane interactions that could cause erroneous results. Each combination was evaluated using the data recorded by the MALS detector. We tested for distinct signals by injecting monodispersed NP suspension (50 and 500 nm, 50 mg L<sup>-1</sup>, injection volume of 30  $\mu$ L). To test for complete size separation we injected a mixture of 50, 100, 200, and 500 nm spheres (each 200 mg L<sup>-1</sup>, 20  $\mu$ L). The settings to run the AF4 system are presented in Table S1; using these, the elution times of the various NP sizes were recorded. In a second step, a monodispersed suspension of 1000 nm spheres (200 mg L<sup>-1</sup>, 10  $\mu$ L) was injected to determine elution time and signal intensity recorded by the MALS detector. A new mixture of all five NP sizes was analysed under different crossflow conditions (0.5, 1, 2, 3, 4 mL min<sup>-1</sup>, Table S1) to test if a simultaneous separation might be feasible or if there had been a transition from the “normal mode” to the “steric mode”. This was done because previous studies have shown that this transition occurs for particle sizes of about 1  $\mu$ m.<sup>47, 51</sup> The MALS detector provides data on the particles’ radii. For a concentration range for particles of 50 and 200 nm (100–0.1 mg L<sup>-1</sup>, 50  $\mu$ L) it was determined when discernible peaks were detected compared to the baseline and when the particle sizes given by the MALS detector matched the supplier’s specifications.

NPs are made of polymers with different densities. To test the effect of different densities on the elution times of particles, we injected monodispersions of 50 nm PS, gold and silver nanoparticles.

**C) Polymer identification** The final polymer characterization was also conducted using two techniques, Pyrolysis GC-MS for NPs and micro-FTIR for MP. Pyrolysis GC-MS was used to determine the presence of polymers in size fractions previously separated by AF4. Lek canal and Lake IJssel surface waters were examined using pyrolysis GC-MS. To do so, pyrolysis tubes were

filled with 12.5  $\mu$ L sampled water, and the water evaporated at 60°C. This step was repeated resulting in a total sample volume of 25  $\mu$ L. The sample from the Lek canal was tested solely for PS (200 nm) that had been added at concentrations of 0.6 mg L<sup>-1</sup> (mimicking the status before crossflow ultrafiltration), 117 mg L<sup>-1</sup> (after crossflow ultrafiltration) and 1200 mg L<sup>-1</sup>, resulting in PS masses of 15 ng, 3  $\mu$ g and 30  $\mu$ g within the sample volumes of 25  $\mu$ L. These tubes were pyrolysed several times (Table S2) to ascertain whether full material pyrolysis occurred and, if so, when. The analysis focussed on characteristic PS degradation products: styrene (mass 104) and tristyrene (mass 312).<sup>34</sup> Fischer and Scholz-Böttcher<sup>34</sup> showed that the more abundant styrene is non-specific, since it is also produced when chitin is pyrolysed. In contrast, the tristyrene is less abundant, but specific for the presence of PS.

Finally, PS was added to organic rich surface water yielding in PS concentrations of 1 to 20 mg L<sup>-1</sup>. Pyrolysis tubes were filled with 25  $\mu$ L of these solutions, and thus contained 25 to 500 ng PS. The limit of detection (LOD) was determined based on an S/N ratio of 3; the limit of quantification (LOQ) was assessed considering an S/N ratio of 10.

A fragment of the glass fibre filter that contained the solids from a surface water sample from Lake IJssel was cut out, placed in a pyrolysis tube, analysed under the same conditions described above (Tables S2, S3) and examined for the presence of PS.

The second technique used was micro-FTIR to identify MP. In order to measure MP down to 20  $\mu$ m in a feasible time frame, when using micro-FTIR equipped with a single MCT detector, we tested filter surface chemical mapping at two spectral and spatial resolutions. For all measurements, the aperture size was set at 50 x 50  $\mu$ m. The spatial resolution, i.e. the step sizes between measurement points, was set at 20 or 35  $\mu$ m. In combination with the changed step sizes, we tested a spectral resolution of 8 cm<sup>-1</sup> with four scans per point and of 16 cm<sup>-1</sup> with one scan per point (ultra-fast mapping option). To do so, PS fragments (9 to 90  $\mu$ m) were spread on an Anodisc filter. The area of the mapped filter area covered with PS as well as the particle numbers were determined using Picta software.

Using a spatial resolution of 20  $\mu$ m and a spectral resolution of 16 cm<sup>-1</sup>, the surface water sample of Lake IJssel (317 L) was analysed. During a measurement time of 8 hours, four pre-determined fields were mapped, together representing a third of the total filter area. For each mapped field a false colour image was produced using two polymer-specific regions, i.e. between 1480–1430 cm<sup>-1</sup> (C–H bending, aromatic ring stretching) and between 1790–1700 cm<sup>-1</sup> (C=O stretching),<sup>28</sup> in which the colour scheme was proportional to the area above or below the baseline. All potential MP particles were marked and their spectra compared manually to spectra from a library. Particle colours and sizes were recorded at the same time.

## 4. Results

The tested and adapted techniques and the results generated are presented below.

### 4.1 NP recovery using crossflow ultrafiltration

The recovery rates of NP and MP particles were evaluated after concentrating drinking water samples by crossflow ultrafiltration. The three samples revealed an MP recovery of 50.2% ( $\pm 11.9$ ). The NP samples were analysed using AF4-MALS and spectrophotometry and both methods yielded a reproducible NP recovery (Figure 2, Table 1). Spectrophotometry yielded a total NP (50 and 200 nm PS) recovery of 54.0% ( $\pm 2$ ,  $n=3$ ). During AF4 separation the MALS detector revealed that the peak of the 200 nm spheres was less intense, broader and lagged behind after crossflow concentration. The 50 nm NP hardly peaked (Figure 2). The recovery rates calculated using the AUCs were 49.3% ( $\pm 3.7$ ,  $n=3$ ) for the 200 nm particles and 12.7% ( $\pm 1.3$ ,  $n=3$ ) for the 50 nm spheres, which together makes a total NP recovery of 61.9% ( $\pm 4.6$ ,  $n=3$ ) (Table 1). This is higher than the total recovery determined earlier, still acceptable since the values are within the error ranges of the measurements. Further, the MALS detector specified average NP radii of 115 nm ( $\pm 1.5$ ,  $n=125$ ) and 53 nm ( $\pm 2.4$ ,  $n=28$ ) for the concentrated samples and of 111 nm ( $\pm 0.5$ ,  $n=73$ ) and 67 nm ( $\pm 1.9$ ,  $n=19$ ) for the standard suspension analysed (Figure 2). The variations might be attributable to matrix effects yet suggest that homo-aggregation during the concentration was not relevant.

Table 1: Recovery of NP (measured with AF4-MALS and UV-Vis spectrophotometry) and MP after concentrating 100 L of drinking water with crossflow ultrafiltration.

		PS	Recovery (%)	SD
NP	AF4	50 nm	12.7	1.3
		200 nm	49.3	3.7
		total (50+200 nm)	61.9	4.9
	UV	total	54.0	2.0
MP	total	50.2	11.9	

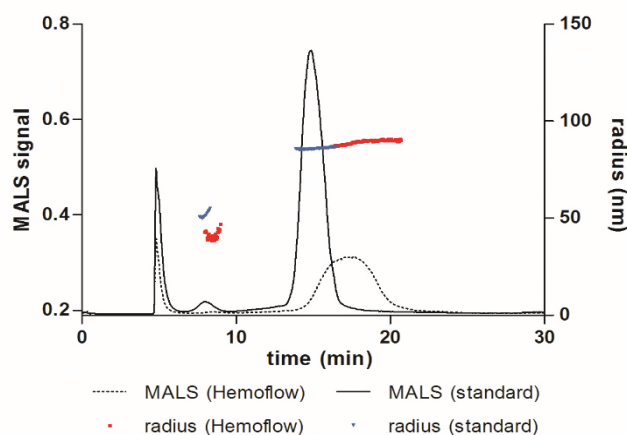


Figure 2: MALS signal and NP radii in drinking water after crossflow ultrafiltration and in the standard suspension containing calculated target concentrations.

### 4.2 Size determination of NP using asymmetrical Flow Field-Flow Fractionation (AF4)

First, two membranes, RC and PES, were tested in combination with different carrier liquids. As only the RC membrane and the 0.01% SDS solution led to distinct peaks and a satisfactory size separation (Table S4), this combination was chosen for further tests. A complete size separation of PS spheres in a polydispersion (50, 100, 200 and 500 nm) was possible. Although the 200 and 500 nm peaks were close, they were still distinguishable (Figure 3A).

In a second step, a monodisperse suspension of 1000 nm spheres (200 mg L<sup>-1</sup>, 10  $\mu$ L) was injected. These particles had a similar elution time as the 200 and 500 nm spheres under crossflow conditions of 2 mL min<sup>-1</sup> (Figure 3B). A new mixture of these five NP sizes was analysed under different crossflow conditions (0.5, 1, 2, 3, 4 mL min<sup>-1</sup>, Table S1) but none of these could fractionate particles of 1000 nm successfully, which implies that transition from the “normal mode” to the “steric mode” occurred, and that prior to analysis, particles larger than 500 nm need to be removed by filtration. The scope of the present study did not allow a further, detailed evaluation of particle fractionation in the steric mode.

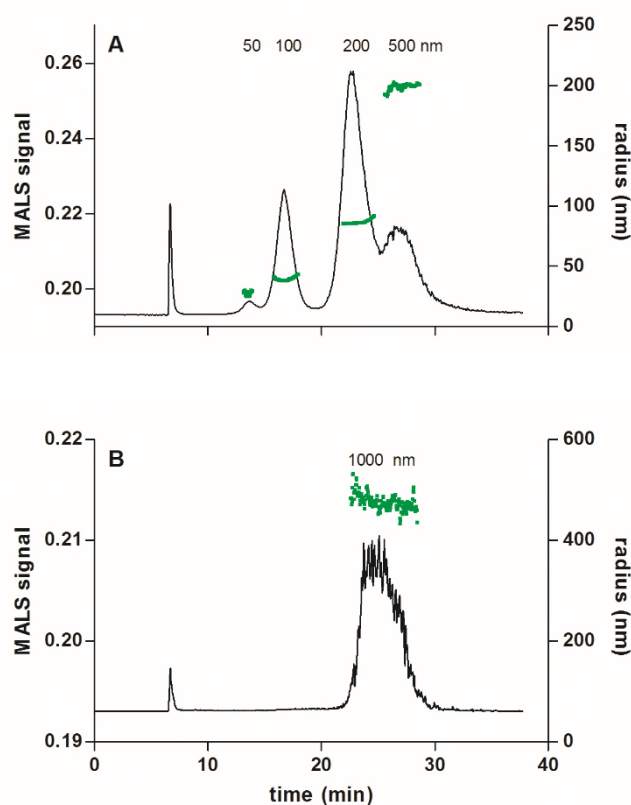


Figure 3: MALS signal (black line) and NP radii (green dots) when analysing (A) a polydispersion of NP (50, 100, 200 and 500 nm) and (B) a monodisperse suspension of NP (1000nm).

The MALS detector indicated average particle sizes of 72 nm ( $\pm 4.3$ ,  $n=23$ ), 103 nm ( $\pm 3.8$ ,  $n=60$ ), 225 nm ( $\pm 4.5$ ,  $n=76$ ) and 514 nm ( $\pm 7.1$ ,  $n=85$ ) (Figure 3A), and further 1233 nm ( $\pm 41.7$ ,  $n=161$ ) (Figure 3B), which fairly matches the characteristics of

originally injected spheres. For particles of 50 and 200 nm ( $100 - 0.1 \text{ mg L}^{-1}$ ,  $50 \mu\text{L}$ ) the concentration range was determined where distinguishable peaks were detected and where particle sizes were in accordance with the supplier's specifications. The particles of 200 nm were still detected correctly at a PS concentration of  $1 \text{ mg L}^{-1}$ , but not at a concentration of  $0.5 \text{ mg L}^{-1}$ . For particles of 50 nm the detection limit was between 5 and  $10 \text{ mg L}^{-1}$ . In combination with pre-concentration using crossflow ultrafiltration, these LODs would further decrease by 200 times, resulting in values between 5 and  $50 \mu\text{g L}^{-1}$ . Lastly, to test the effect of different particle densities on the elution times of particles, monodispersions of 50 nm PS, gold and silver nanoparticles were injected. Using the same settings, the particles eluted at the same time (Figure 4), indicating that different polymer densities will not hinder a satisfactory size fractionation of NP.

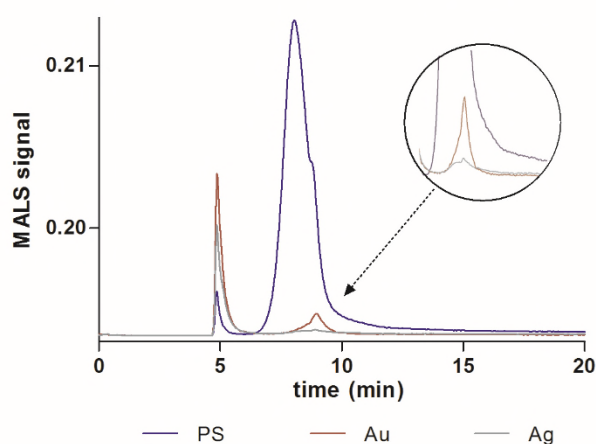


Figure 4: MALS signal revealed similar elution times for nanoparticles (50 nm) made of PS, gold and silver.

#### 4.3 Identification of NP using Pyrolysis GC-MS

First, samples from the Lek canal with added PS masses of 15 ng,  $3 \mu\text{g}$  and  $30 \mu\text{g}$  were analysed and examined for the presence of the styrene (mass 104) and tristyrene (mass 312) (Figure S3). Compared with the values detected for  $3 \mu\text{g}$  PS, the styrene intensity for  $30 \mu\text{g}$  PS was ten times higher but the tristyrene intensity was only twice as high, indicating that pyrolysis of the material was incomplete. Although this does not hamper polymer identification, it might hamper a quantification with one run.

Secondly, pyrolysis tubes containing masses of 25 to 500 ng PS in organic-rich surface water were analysed to ascertain the LOD and LOQ of this method. The styrene was detected in all pyrolysis tubes with lower PS concentrations (Figure S3). The tristyrene was identified for PS of at least 100 ng (S/N ratio of 7). As tristyrene is specific for PS, the analysis should focus on this compound, which will result in an LOD between 50 and 100 ng and an LOQ between 100 and 250 ng for environmental samples. Under the given settings and pyrolysed volumes of  $25 \mu\text{L}$ , an LOD of  $4 \text{ mg L}^{-1}$  and an LOQ of  $4-10 \text{ mg L}^{-1}$  were assessed.

Lastly, the surface water sample from Lake IJssel was analysed and examined for the presence of PS. Both degradation products of PS (styrene and tristyrene) were detected. Based on the previously determined LOD, the sample must have contained at least  $100 \text{ ng}$  ( $4 \text{ mg L}^{-1}$ ) of PS.

#### 4.4 Identification of MP using Micro-FTIR

Using different spectral and spatial resolutions during chemical mapping yielded slightly varying PS-covered areas and particle counts between the step sizes of  $20 \mu\text{m}$  (29 particles and 9.4%; 32 particles and 9.2%) and  $35 \mu\text{m}$  (25 particles and 9.3%; 28 particles and 10.6%). Step sizes of  $20 \mu\text{m}$  were preferred since we aimed to detect small MP for which information would be lost if step sizes were bigger. Further, the smaller step sizes allow a more precise determination of sizes and numbers for particles that lie close to each other. Both spectral resolutions yielded spectra of sufficient quality to identify polymer types. We used the lower spectral resolution for further measurements, since it required shorter measuring times. Based on data generated during micro-FTIR analysis we estimated polymer masses. While the two-dimensional shape of each particle can be assessed, the third dimension required for calculating a particle's mass cannot be measured. We assume that the particle's largest surface area will probably be attached to the filter. Thus, this third dimension can be at a max similar to the determined dimensions for spherical particles, for very thin fragments the value can be near zero. For a large number of particles (e.g.  $n=100$ ), an average third dimension can be estimated as half of the maximum and minimum values. In the Lake IJssel sample, PE particles ( $28$  to  $158 \mu\text{m}$ ) were detected. Following the aforementioned approach, this translates into a total PE concentration in a range from 5 to  $60 \text{ ng L}^{-1}$ .

#### 4.5. Evaluation of the proposed framework

Several techniques are needed in order to determine a wide size range of plastics. The framework we present makes it possible firstly to concentrate on NP and MP, and secondly to identify and quantify the sizes and polymer types of various NPs and MPs in an aqueous environmental matrix. During this study, individual techniques were tested that proved to be promising for application in this field of research (Figure 5). The approach is similar to the one presented recently by Ter Halle, *et al.*<sup>16</sup> who sampled plastic of various sizes in the North Atlantic: They applied micro-FTIR for MP detection  $> 25 \mu\text{m}$  and a combination of dynamic light scattering (DLS) and pyrolysis GC-MS to identify NP.

Compared to the techniques' theoretical size constraints as presented in Figure 1, only slight adaptations needed to be made (Figure 5). Using a micro-FTIR that is not equipped with an advanced focal plane array detector which can measure several pixels at the same time<sup>28, 51</sup> we suggest mapping the surface of a filter in steps of  $20 \mu\text{m}$  at a reduced spectral resolution. This enables MP down to  $28 \mu\text{m}$  to be determined. To assess polymer masses from the generated results, we propose a particle shape analysis. Although based on an assumption about the particles' third dimension, this approach offers a solution

for combining MP and NP data not only within the framework presented, but also in studies in general.

NP particles are examined using a combination of AF4-MALS and pyrolysis GC-MS. The AF4-MALS was tested and the settings optimized to allow NP between 50 and 500 nm to be separated. Based on these settings and depending on the particle sizes, the coupled MALS detector detected particle sizes for PS concentrations of 1–10 mg L<sup>-1</sup>. In our approach, the AF4-MALS sample fractionation is based on previously determined elution times and thus, is not concentration-dependent. Subsequently, individual fractions are analysed using pyrolysis GC-MS. Although there is no size limitation, a minimum of approximately 100 ng is required to guarantee the detection of PS in an environmental matrix. Based on the analysed sample volume of 25 µL, a concentration of 4 mg L<sup>-1</sup> PS would be required.

To decrease the LODs, particles need to be concentrated during sampling. To do so, we introduced crossflow ultrafiltration using a Hemoflow filter and determined that NP were recovered reproducibly for sample volumes of 100 L. At a concentration factor of 200, the LOD for originally present particles would decrease to 20 µg L<sup>-1</sup>. Recommendations for addressing the remaining “gaps” in the NP – MP size continuum (dashed lines, Figure 5) of the proposed framework are discussed below.

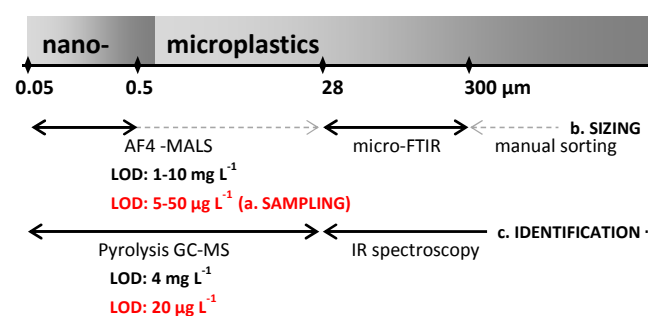


Figure 5: Overview of techniques applied, showing respective size and concentration limitations. Using a crossflow filter, particles were concentrated by a factor of 200, which further decreased the LODs.

## 5. Discussion

### 5.1 Closing the gaps

The field of MP and NP research is relatively young, implying that methods are still under development. So far, the use of FTIR or Raman microscopy has been favoured for the examination of MP at micrometre sizes. Although these techniques enable sizes, shapes and polymer types to be detected simultaneously, they have shortcomings regarding detectable particle sizes, their semi-quantification and their long measurement and data analysis times. As previous studies<sup>16, 28</sup> have noted, it is preferable to analyse whole samples, especially if they are very heterogeneous. However, this is laborious and time-consuming. Of great benefit is an automatic approach to handle data generated by micro-FTIR, reducing the workload and increasing objectivity and comparability of the data generated.<sup>52</sup> In addition, the particle shape analysis we

propose enables the relationship between data derived from spectroscopic and thermal degradation methods to be ascertained. Recently, polymer mixtures in environmental matrices have been determined using thermogravimetric analysis (TGA),<sup>31</sup> or pyrolysis<sup>16, 33</sup> coupled to a GC-MS system. A TGA system offers controlled continuous heating with a simultaneous weight loss determination and sample volumes of 20 mg soil.<sup>31</sup> Using pyrolysis GC-MS and sample volumes of 1 mg, Fischer and Scholz-Böttcher<sup>33</sup> evaluated the LOD and LOQ for various polymer types in fish samples and were constrained only by the scale used (repeatability of 0.25 µg). They therefore expect these limits to lie in the range of nanograms, which makes thermal degradation methods appealing for detecting NP.

As already mentioned, MP and NP sizes should be routinely provided, due to size-related effects<sup>45</sup> and to enable comparisons with other studies. Using AF4 and analysing individual size fractions generates broad and valuable results.

This could complement the protocol proposed by Ter Halle, *et al.*<sup>16</sup> using DLS and pyrolysis GC-MS. In comparison with DLS, the size determination using AF4-MALS is not concentration-dependent but is based on a priori determined elution times of injected NP standards (Figure 3A). Applying DLS for heterogeneous samples might cause misinterpretation of particle sizes and an underestimation of very small particles.<sup>47</sup> The different polymer densities will not hinder a satisfactory separation, as separation is dependent on particle sizes, not densities. We did not elaborate on the particle fractionation in the steric mode, but after Dou, *et al.*<sup>54</sup> separated PS spheres from 1 µm up to 40 µm satisfactorily, we conclude the AF4 being appropriate to fill the remaining gap in the proposed protocol (Figure 5).

### 4.3 Sampling and sample preparation

Adequate sampling of NP to reach methodological detection limits of further analyses is especially challenging. We propose using (Hemoflow) crossflow ultrafiltration to concentrate NP. To evaluate this technique, we tested NP recovery and potential aggregation processes. Although reproducible, the recovery of the 50 nm spheres was not yet at its full potential (Table 1). Hemoflow crossflow filters are used as dialysis equipment and are made to retain proteins of 60 kDa. SEM microscopy might be used to test if damaged membranes were limiting the recovery of 50 nm spheres, or if the current limitation could be attributed to attachments on the inner walls of the equipment used. Doses of a surfactant in low concentrations might reduce particle–membrane and attachment interactions and subsequently increase the recovery rates. Further, we demonstrate the potential of the this crossflow ultrafiltration setup for sampling surface waters: 635 L were filtered and the particles concentrated into a volume of 0.4 L, which corresponds to a concentration factor of 1580. This might be increased by a subsequent ultrafiltration.<sup>16</sup> Ter Halle, *et al.*<sup>16</sup> concentrated surface water samples of 1 L using ultrafiltration in a polysulfone-based cell. The filtration had to be repeated several times because the cell volume was 180 ml, but they

finally succeeded in reducing the sample volume to 10 ml – a concentration factor of 200.

Although we tested the fibrous Hemoflow membranes with an inner diameter of approximately 200 µm for filtering MP of 100 µm size, we suggest to combine conventional filtration, e.g. with stacked sieves, with crossflow ultrafiltration (Figure S1). Using sieves of e.g. 20 µm, 300 µm and 1 mm allows for large volumes of water to be filtered, as larger particles would no longer clog the membrane of the Hemoflow.

A further point to consider is sample preparation. This is already laborious for MP, but will be extremely challenging for NP. Several approaches have been presented for MP, but studies are now focusing on an enzymatic<sup>25, 33, 55-57</sup> or alkaline<sup>50, 58, 59</sup> treatment to reduce the organic sample matrix while inorganic particles are removed due to their higher density.

## Conclusion and outlook

The presented analytical framework aims to contribute to a more consistent determination of a broad size spectrum of plastic particles, including NP, in aqueous environmental samples. We have shown empirical data on the applicability of the techniques used to sample, to determine plastic sizes and to identify polymer types. The sampling is especially challenging for NP, but crossflow ultrafiltration proved to reproducibly concentrate NP. By doing so, it completes conventional filtration methods, and could be complemented by further ultrafiltration.<sup>16</sup>

The data this framework generates will help elucidate environmental fate (including fragmentation processes), will allow a system-based mass balance to be achieved and, ultimately, will allow assessing environmental risks of MP and NP.

## Conflicts of interest

There are no conflicts to declare.

## Acknowledgements

This study was funded by the Dutch Technology Foundation TTW (project number 13940). We acknowledge additional support from and discussions with representatives from KWR, IMARES, NVWA, RIKILT, the Dutch Ministry of Infrastructure and the Environment, The Dutch Ministry of Health, Welfare and Sport, Wageningen Food & Biobased Research, STOWA, RIWA, and the Dutch water boards. This study was conducted within the framework of the joint research program (BTO) of Dutch water companies and the Belgian De Watergroep. Thanks to J. Burrough for advising on the English.

## References

1. T. Mani, A. Hauk, U. Walter and P. Burkhardt-Holm, *Scientific Reports*, 2015, **5**, 1-7.
2. K. L. Law, S. E. Moret-Ferguson, D. S. Goodwin, E. R. Zettler, E. De Force, T. Kukulka and G. Proskurowski, *Environmental science & technology*, 2014, **48**, 4732-4738.
3. A. Cozar, F. Echevarria, J. I. Gonzalez-Gordillo, X. Irigoien, B. Ubeda, S. Hernandez-Leon, A. T. Palma, S. Navarro, J. Garcia-de-Lomas, A. Ruiz, M. L. Fernandez-de-Puelles and C. M. Duarte, *Proceedings of the National Academy of Sciences of the United States of America*, 2014, **111**, 10239-10244.
4. S. Kühn, E. L. Bravo Rebolledo and J. A. Van Franeker, in *Marine Anthropogenic Litter*, eds. M. Bergmann, L. Gutow and M. Klages, Springer, Berlin, 2015, ch. 4, pp. 75-116.
5. C. B. Jeong, E. J. Won, H. M. Kang, M. C. Lee, D. S. Hwang, U. K. Hwang, B. Zhou, S. Souissi, S. J. Lee and J. S. Lee, *Environmental science & technology*, 2016, **50**, 8849-8857.
6. C. Arthur, J. Baker and H. Bamford, 2009.
7. A. J. Verschoor, *Towards a definition of microplastics - Considerations for the specification of physico-chemical properties*, National Institute for Public Health and the Environment, Bilthoven, The Netherlands, 2015.
8. A. A. Koelmans, E. Besseling and W. J. Shim, in *Marine Anthropogenic Litter*, eds. M. Bergmann, L. Gutow and M. Klages, Springer International Publishing, Cham, 2015, DOI: 10.1007/978-3-319-16510-3\_12, pp. 325-340.
9. L. M. Hernandez, N. Yousefi and N. Tufenkji, *Environmental Science & Technology Letters*, 2017, **4**, 280-285.
10. B. Gewert, M. M. Plassmann and M. MacLeod, *Environmental Science-Processes & Impacts*, 2015, **17**, 1513-1521.
11. S. Lambert and M. Wagner, *Chemosphere*, 2016, **145**, 265-268.
12. J. Gigault, B. Pedrono, B. Maxit and A. Ter Halle, *Environmental Science-Nano*, 2016, **3**, 346-350.
13. Y. K. Song, S. H. Hong, M. Jang, G. M. Han, S. W. Jung and W. J. Shim, *Environmental science & technology*, 2017, **51**, 4368-4376.
14. J. E. Weinstein, B. K. Crocker and A. D. Gray, *Environmental Toxicology and Chemistry*, 2016, **35**, 1632-1640.
15. A. A. Koelmans, M. Kooi, K. L. Law and E. v. Seville, *Environmental Research Letters*, 2017, **12**.
16. A. Ter Halle, L. Jeanneau, M. Martignac, E. Jardé, B. Pedrono, L. Brach and J. Gigault, *Environmental science & technology*, 2017, DOI: 10.1021/acs.est.7b03667.
17. K. Mattsson, L. A. Hansson and T. Cedervall, *Environmental Science-Processes & Impacts*, 2015, **17**, 1712-1721.
18. J. P. da Costa, P. S. M. Santos, A. C. Duarte and T. Rocha-Santos, *Science of the Total Environment*, 2016, **566**, 15-26.
19. M. Wagner, C. Scherer, D. Alvarez-Muñoz, N. Brennholt, X. Bourrain, S. Buchinger, E. Fries, C. Grosbois, J. Klasmeier, T. Marti, S. Rodriguez-Mozaz, R. Urbatzka, A. D. Vethaak, M. Winther-Nielsen and G. Reifferscheid, *Environmental Sciences Europe*, 2014, **26**, 1-9.
20. M. Filella, *Environmental Chemistry*, 2015, **12**, 527-538.
21. M. Eriksen, S. Mason, S. Wilson, C. Box, A. Zellers, W. Edwards, H. Farley and S. Amato, *Marine pollution bulletin*, 2013, **77**, 177-182.
22. V. Hidalgo-Ruz, L. Gutow, R. C. Thompson and M. Thiel, *Environmental science & technology*, 2012, **46**, 3060-3075.
23. S. A. Carr, J. Liu and A. G. Tesoro, *Water Research*, 2016, **91**, 174-182.
24. S. Ziajahromi, P. A. Neale, L. Rintoul and F. D. L. Leusch, *Water Research*, 2017, **112**, 93-99.
25. S. M. Mintenig, I. Int-Veen, M. G. J. Löder, S. Primpke and G. Gerdt, *Water Research*, 2017, **108**, 365-372.

26. H. R. Veenendaal and A. J. Brouwer-Hanzens, *A method for the concentration of microbes in large volumes of water*, 2007.
27. M.-T. Nuelle, J. H. Dekiff, D. Remy and E. Fries, *Environmental Pollution*, 2014, **184**, 161-169.
28. M. G. J. Löder, M. Kuczera, S. Mintenig, C. Lorenz and G. Gerdt, *Environmental Chemistry*, 2015, **12**, 563-581.
29. A. Käßler, F. Windrich, M. G. J. Loder, M. Malanin, D. Fischer, M. Labrenz, K. J. Eichhorn and B. Voit, *Analytical and Bioanalytical Chemistry*, 2015, **407**, 6791-6801.
30. H. K. Imhof, C. Laforsch, A. C. Wiesheu, J. Schmid, P. M. Anger, R. Niessner and N. P. Ivleva, *Water Research*, 2016, **98**, 64-74.
31. E. Dümichen, P. Eisentraut, C. G. Bannick, A.-K. Barthel, R. Senz and U. Braun, *Chemosphere*, 2017, **174**, 572-584.
32. M. Majewsky, H. Bitter, E. Eiche and H. Horn, *Science of the Total Environment*, 2016, **568**, 507-511.
33. M. Fischer and B. M. Scholz-Böttcher, *Environmental science & technology*, 2017, DOI: 10.1021/acs.est.6b06362.
34. E. Dümichen, A.-K. Barthel, U. Braun, C. G. Bannick, K. Brand, M. Jekel and R. Senz, *Water Research*, 2015, **85**, 451-457.
35. S. M. E. Cannon, J. L. Lavers and B. Figueiredo, *Mar Pollut Bull*, 2016.
36. Y. K. Song, S. H. Hong, M. Jang, G. M. Han, M. Rani, J. Lee and W. J. Shim, *Marine pollution bulletin*, 2015, **93**, 202-209.
37. M. R. Twiss, *Journal of Great Lakes Research*, 2016.
38. A. McCormick, T. J. Hoellein, S. A. Mason, J. Schlupe and J. J. Kelly, *Environmental science & technology*, 2014, **48**, 11863-11871.
39. A. Collignon, J. H. Hecq, F. Galgani, F. Collard and A. Goffart, *Marine pollution bulletin*, 2014, **79**, 293-298.
40. A. Vianello, A. Boldrin, P. Guerriero, V. Moschino, R. Rella, A. Sturaro and L. Da Ros, *Estuarine, Coastal and Shelf Science*, 2013, **130**, 54-61.
41. M. Claessens, S. De Meester, L. Van Landuyt, K. De Clerck and C. R. Janssen, *Marine pollution bulletin*, 2011, **62**, 2199-2204.
42. H. A. Leslie, S. H. Brandsma, M. J. M. van Velzen and A. D. Vethaak, *Environment International*, 2017, **101**, 133-142.
43. H. Bouwmeester, P. C. H. Hollman and R. J. B. Peters, *Environ Sci Technol*, 2015, **49**, 8932-8947.
44. A. A. Koelmans, N. J. Diepens, I. Velzeboer, E. Besseling, J. T. K. Quik and D. van de Meent, *Science of the Total Environment*, 2015, **535**, 141-149.
45. P. E. Redondo-Hasselerharm, D. Falahudin, E. T. H. M. Peeters and A. A. Koelmans, *Environmental science & technology*, 2018, DOI: 10.1021/acs.est.7b05367.
46. A. A. Koelmans, E. Besseling, E. Foekema, M. Kooi, S. Mintenig, B. C. Ossendorp, P. E. Redondo-Hasselerharm, A. Verschoor, A. P. van Wezel and M. Scheffer, *Environmental science & technology*, 2017, **51**, 11513-11519.
47. J. Gigault, H. El Hadri, S. Reynaud, E. Deniau and B. Grassl, *Analytical and Bioanalytical Chemistry*, 2017, **409**, 6761-6769.
48. L. J. Gimbert, K. N. Andrew, P. M. Haygarth and P. J. Worsfold, *Trac-Trends in Analytical Chemistry*, 2003, **22**, 615-633.
49. F. A. Messaud, R. D. Sanderson, J. R. Runyon, T. Otte, H. Pasch and S. K. R. Williams, *Progress in Polymer Science*, 2009, **34**, 351-368.
50. A. Dehaut, A.-L. Cassone, L. Frère, L. Hermabessiere, C. Himber, E. Rinnert, G. Rivière, C. Lambert, P. Soudant, A. Huvet, G. Duflos and I. Paul-Pont, *Environmental Pollution*, 2016, **215**, 223-233.
51. A. S. Tagg, M. Sapp, J. P. Harrison and J. J. Ojeda, *Analytical Chemistry*, 2015, **87**, 6032-6040.
52. S. Primpke, C. Lorenz, R. Rascher-Friesenhausen and G. Gerdt, *Analytical Methods*, 2017, **9**, 1499-1511.
53. P. Herrero, P. S. Bauerlein, E. Emke, E. Pocurull and P. de Voogt, *Journal of Chromatography A*, 2014, **1356**, 277-282.
54. H. Dou, Y. J. Lee, E. C. Jung, B. C. Lee and S. Lee, *Journal of Chromatography A*, 2013, **1304**, 211-219.
55. M. Cole, H. Webb, P. Lindeque, E. S. Fileman, C. Halsband and T. S. Galloway, *Scientific Reports*, 2014, **4**, 1-8.
56. W. Courteney-Jones, B. Quinn, F. Murphy, S. F. Gary and B. E. Narayanaswamy, *Analytical Methods*, 2017, DOI: 10.1039/C6AY02343F.
57. M. G. J. Löder, H. K. Imhof, M. Ladehoff, L. A. Löschel, C. Lorenz, S. Mintenig, S. Piehl, S. Primpke, I. Schrank, C. Laforsch and G. Gerdt, *Environmental science & technology*, 2017, DOI: 10.1021/acs.est.7b03055.
58. S. Kühn, B. van Werven, A. van Oyen, A. Meijboom, E. L. Bravo Rebolledo and J. A. van Franeker, *Marine pollution bulletin*, 2017, **115**, 86-90.
59. E. Hermsen, R. Pompe, E. Besseling and A. A. Koelmans, *Marine pollution bulletin*, 2017, **122**, 253-258.

## Closing the gap between small and smaller: Towards a framework to analyse nano- and microplastics in aqueous environmental samples

Svenja M. Mintenig <sup>a,b</sup>, Patrick S. Bäuerlein <sup>b</sup>, Albert A. Koelmans <sup>c,d</sup>, Stefan C. Dekker <sup>a,e</sup>, Annemarie P. van Wezel <sup>a,b</sup>

<sup>a</sup> Copernicus Institute of Sustainable Development, Utrecht University, The Netherlands.

<sup>b</sup> KWR Watercycle Research Institute, Nieuwegein, The Netherlands.

<sup>c</sup> Aquatic Ecology and Water Quality Management Group, Wageningen University, The Netherlands.

<sup>d</sup> Wageningen Marine Research, IJmuiden, The Netherlands.

<sup>e</sup> Faculty of Management, Science and Technology, Open University, Heerlen, The Netherlands

### Supporting Information

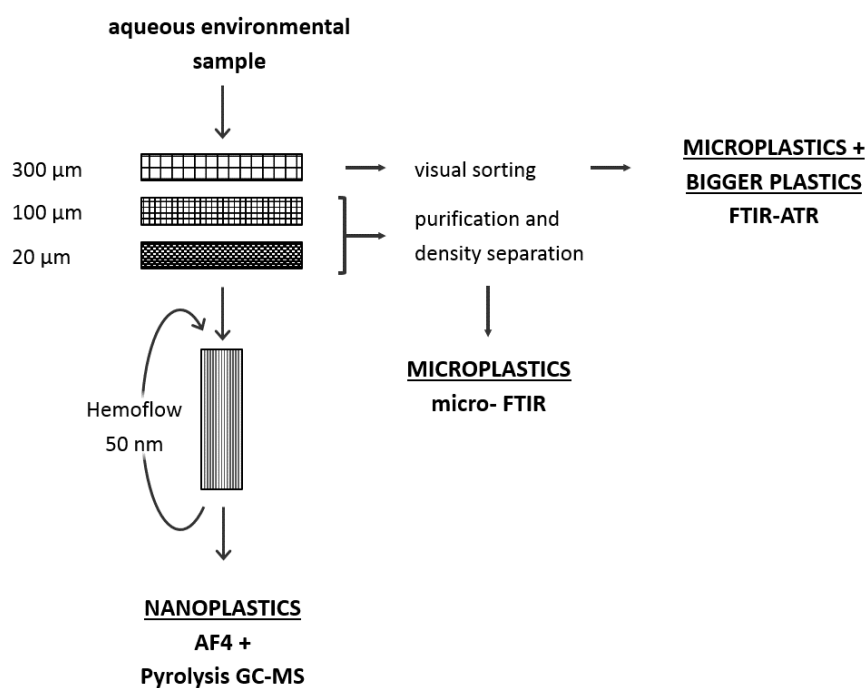


Figure S 1: Scheme of combined techniques to sample and analyse nano- and microplastics.

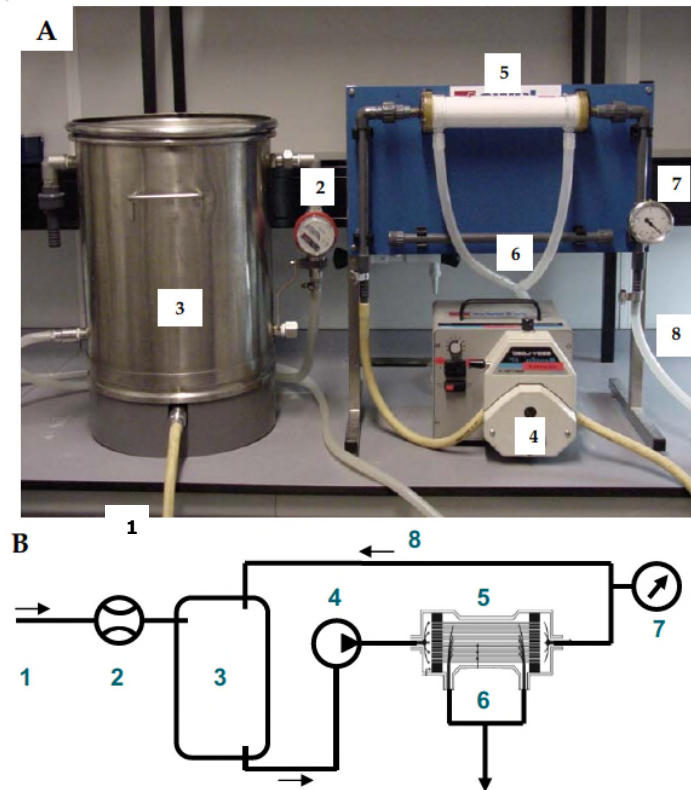


Figure S 2: Schematic presentation of the Hemoflow crossflow ultrafiltration. 1 = water inflow, 2 = water meter, 3 = tank with float valve, 4 = pump, 5 = Hemoflow filter, 6 = permeate, 7 = pressure gauge, 8 = concentrate, circulation back into (3) tank (Source: Veenendaal and Brouwer-Hanzens <sup>1</sup>).

Table S 1: Settings used at the AF4. For the separation of a NP mixture different crossflows were tested.

	Tested Settings (membrane & carrier liquid)	Applied Settings
Membrane	Reg. cellulose (RC) 10 kDa	RC
Carrier liquid	Polyethersulfone (PES) 10 kDa Milli-Q 0.01% SDS 0.01% TWEEN	0.01% SDS
Spacer thickness	250 $\mu\text{m}$	250 $\mu\text{m}$
Detector flow	1.0 ml min <sup>-1</sup>	1.0 ml min <sup>-1</sup>
Split flow	0 ml min <sup>-1</sup>	0 ml min <sup>-1</sup>
Cross flow	1.5 ml min <sup>-1</sup> (0-11 min) 1.5-0 ml min <sup>-1</sup> (11-50 min, exp. 0.2) 0 ml ml min <sup>-1</sup> (50-65 min)	1 ml min <sup>-1</sup> (0-8 min) 1-0 ml min <sup>-1</sup> (8-28 min, exp. 0.2) 0 ml min <sup>-1</sup> (28-33 min)
Focusing flow	2.3 ml min <sup>-1</sup>	1.8 ml min <sup>-1</sup>
Injection flow	0.2 ml min <sup>-1</sup>	0.2 ml min <sup>-1</sup>
Injection time	6 min	4 min
Injection volume	30 $\mu\text{l}$ (monodispersed) (10 $\mu\text{l}$ PS polydispersion)	50 $\mu\text{l}$

**Table S 2: Settings to run the pyrolysis of the samples.**

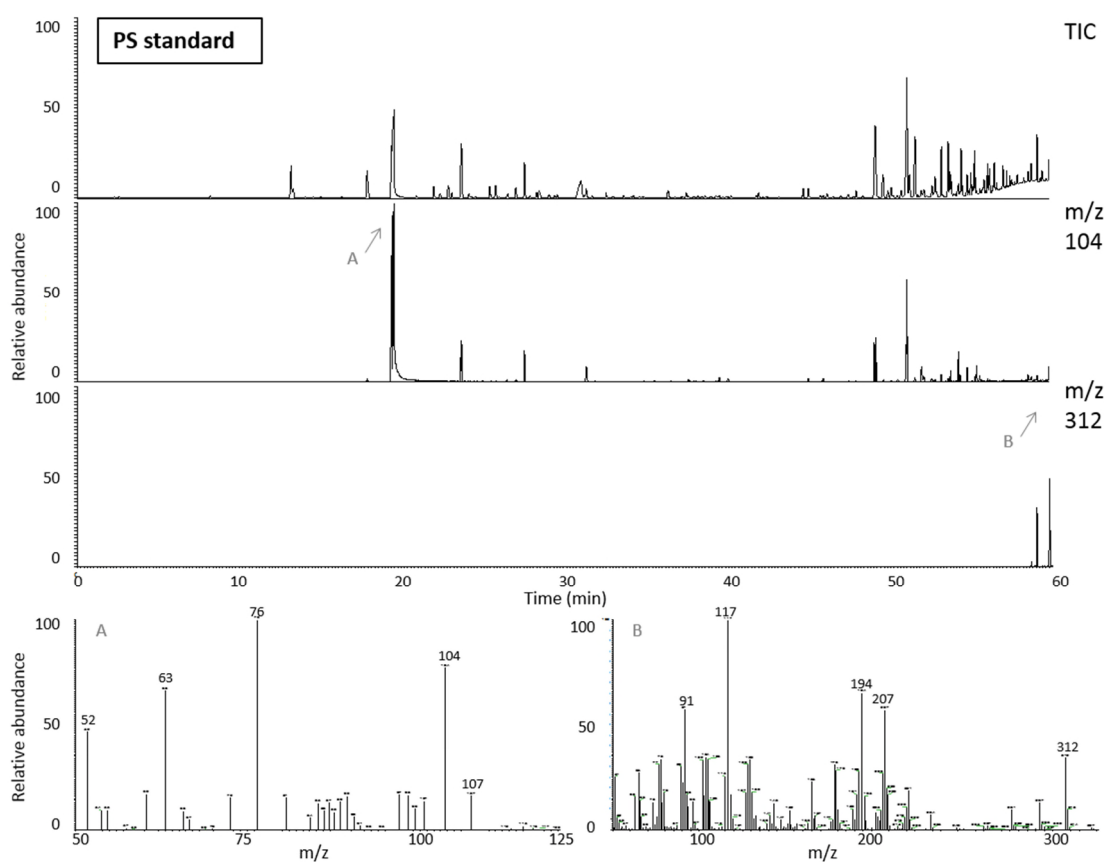
General timing:	
Clean time	20.0 s
Clean time #2	60.0 s
Delay time	0.0 min
Equilibration time	20.0 s
Standby Temperature	
Head temperature	150.0 °C
Offset AS	50.0 °C
Default Parameters	
Temperature	150.0 °C
Pyro Time	10.0 s
Table	single
Pyrolysis Cup	560 °C

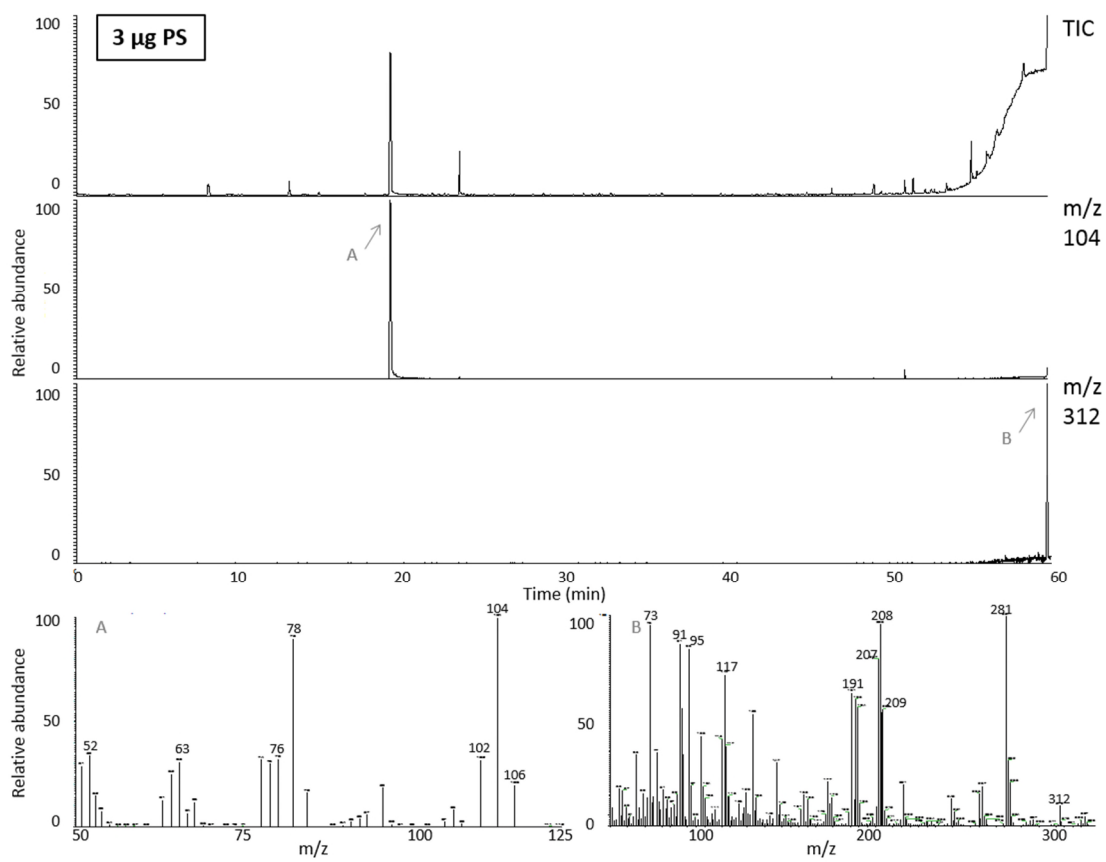
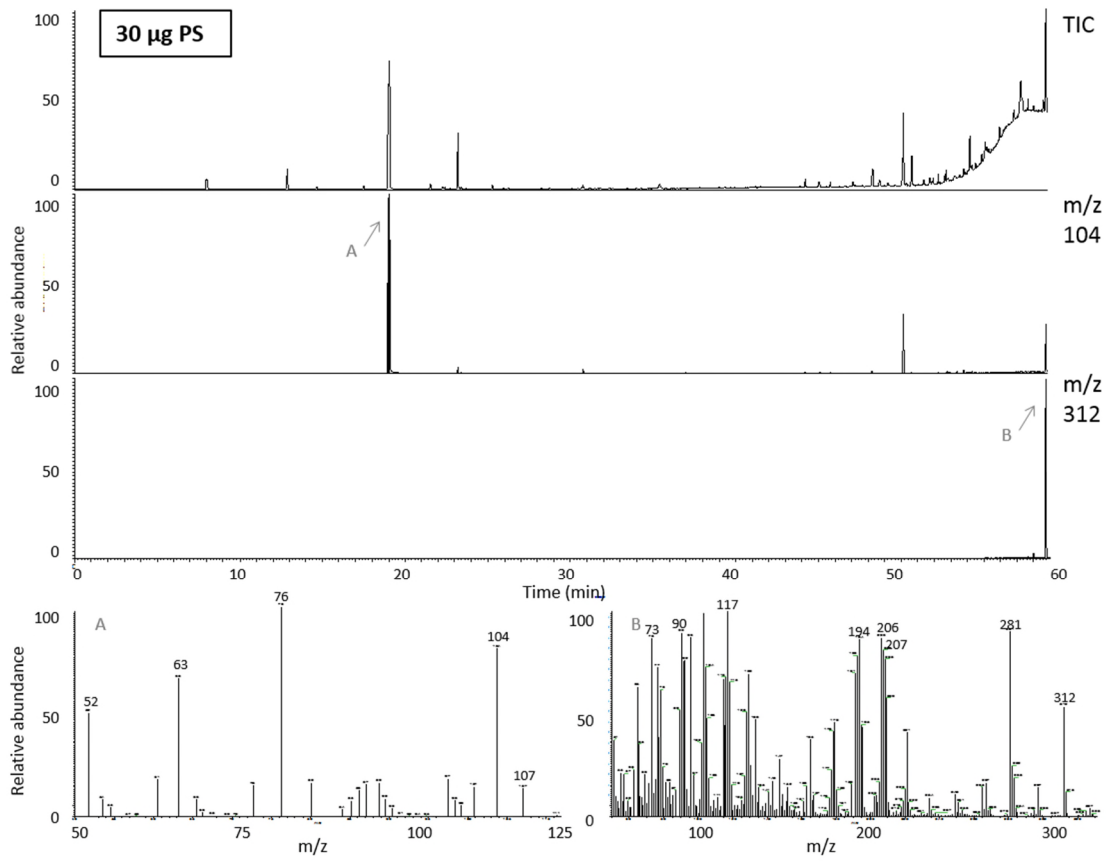
**Table S 3: Settings to run the GC-MS.**

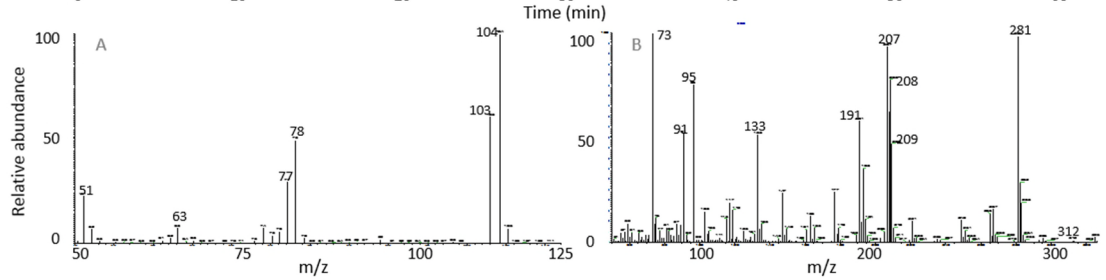
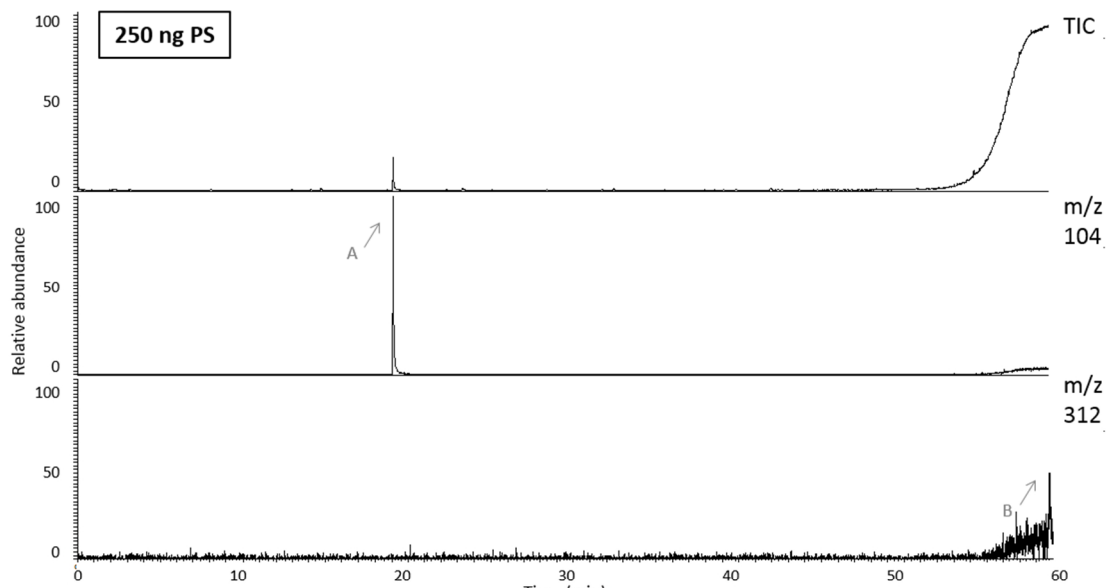
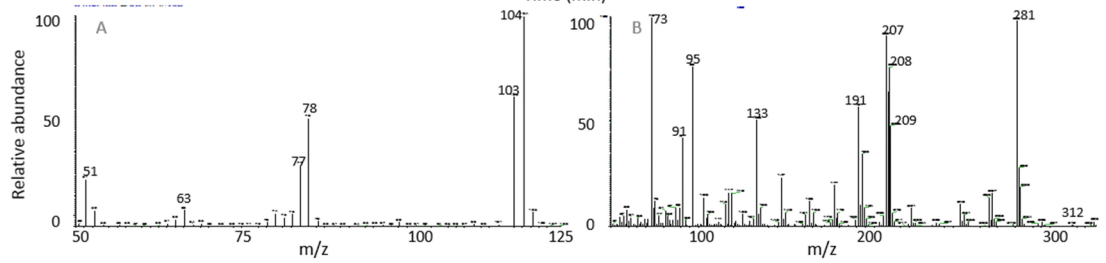
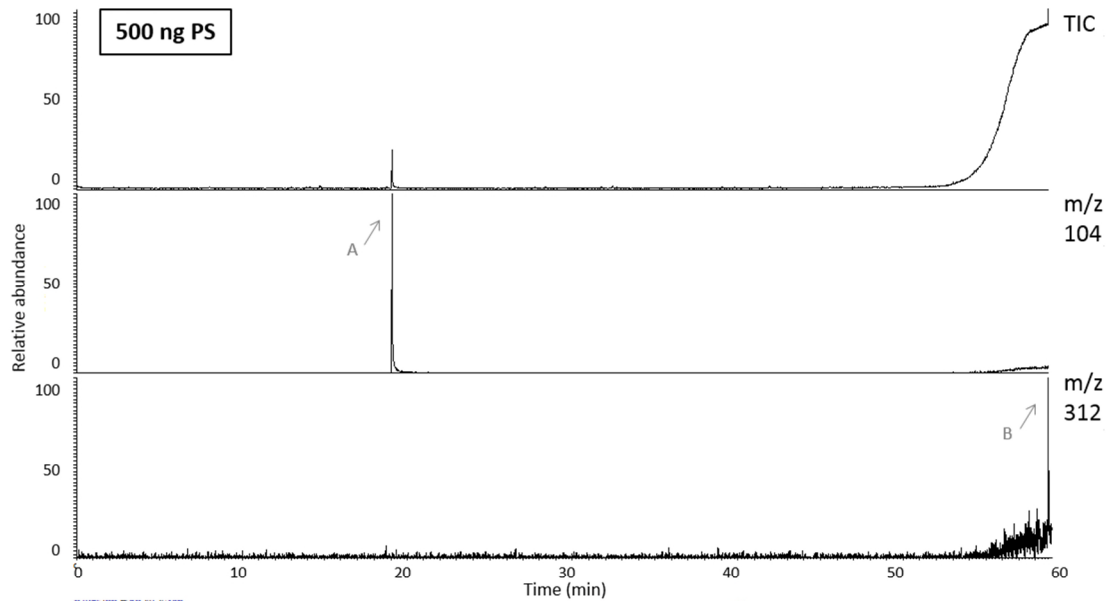
Oven	
Initial Temperature	40 °C
Initial Time	4.00 min
Number of Ramps	2
Rate #1	4.0 °C/min
Final Temperature #1	230 °C
Hold Time #1	0.00 min
Rate #2	20.0 °C/min
Final Temperature #2	325 °C
Hold Time #2	5.00 min
Maximum Temperature	350 °C
Prep Run Timeout	10.00 min
Equilibration Time	0.50 min
Inlet	
Mode	split
Base Temperature	200 °C
Split Flow	40 ml/min
Split ratio	10
Carrier	
Mode	Constant flow
Initial Value	4.00 ml/min
Detector	
Mode	Full scan
Mass Range	50 – 1000 amu
Time Range	0 – 59 min
Peak Format	Centriod
Scan Time	0.40 s
Multiplier	600 V
Ionisation Mode	EI+
Source Temperature	200 °C
Interface Temperature	280 °C

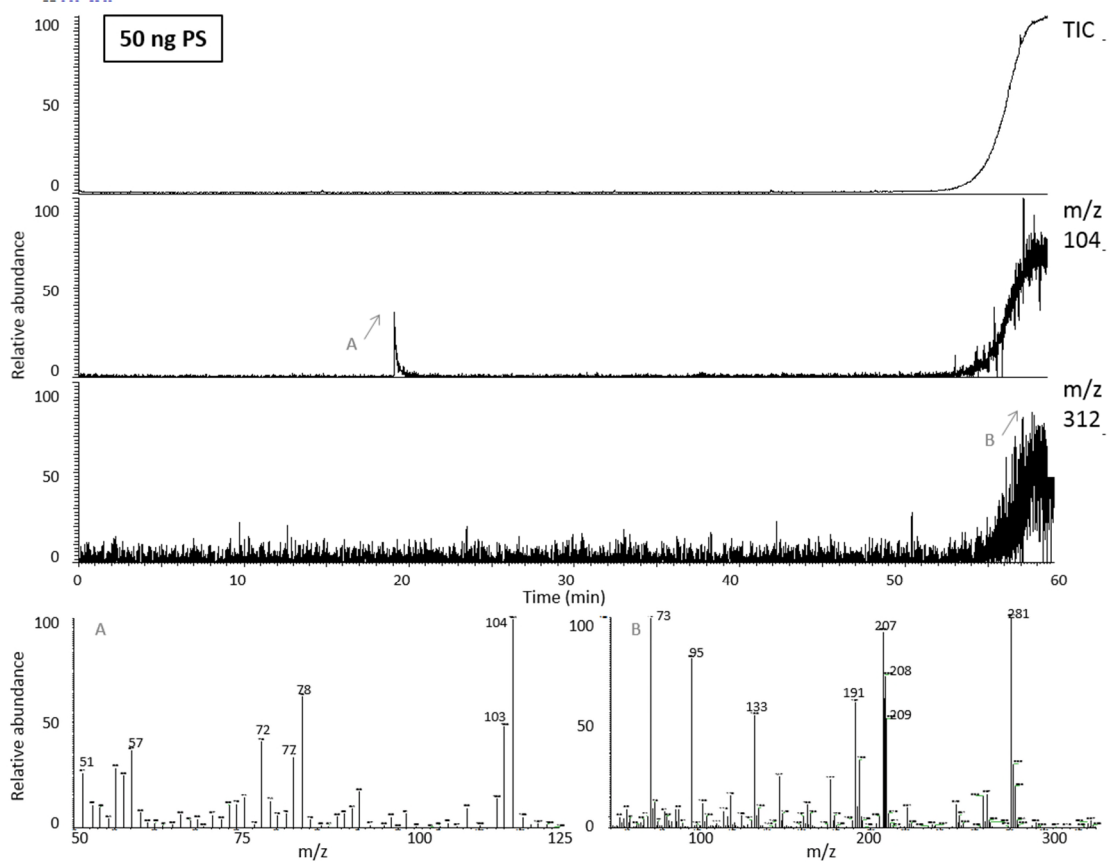
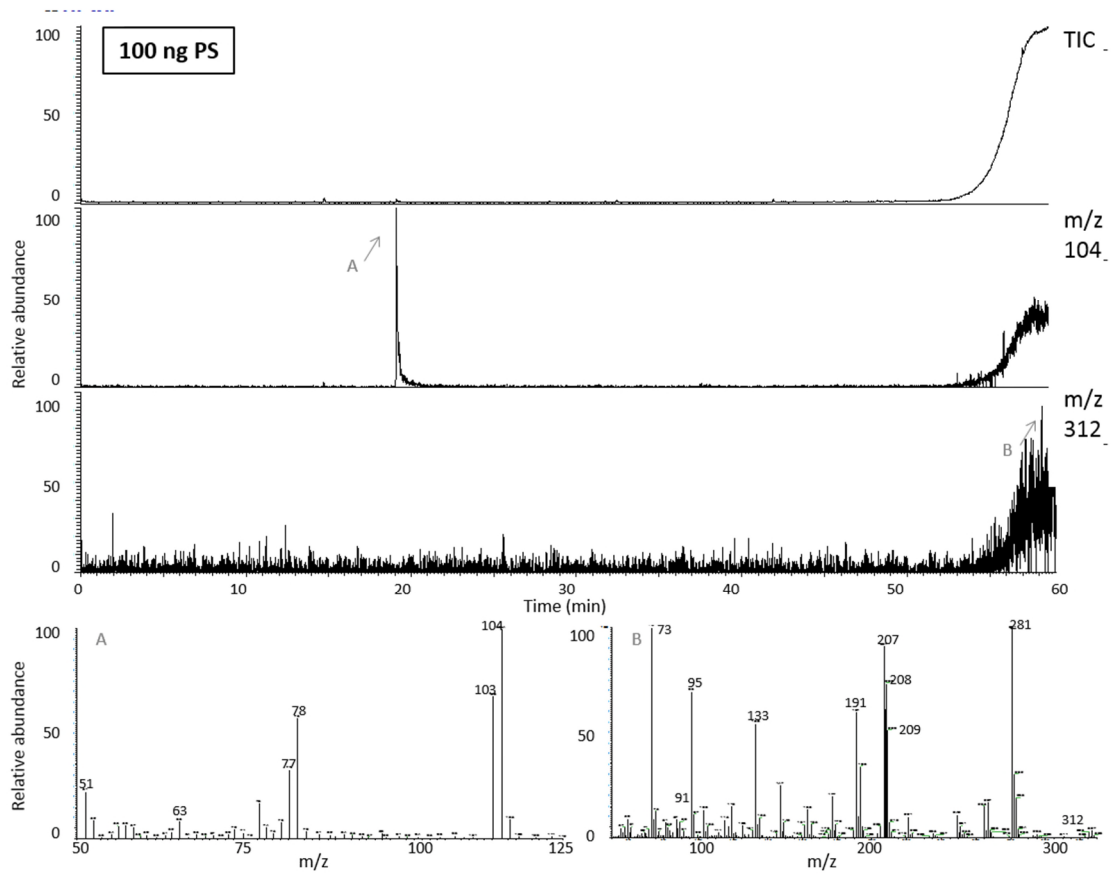
**Table S 4: Separation efficiency for various AF4 membrane/ carrier liquid combinations. The fractionation of mono- and polydispersed solutions was concerned successful (marked with an “Y”) when resulting in clear distinct peaks.**

	50 nm	500 nm	fractionation of mixture
PES & Milli-Q	Y	Y	-
PES & SDS	-	-	-
PES & TWEEN	-	-	-
RC & Milli-Q	(y)	Y	-
RC & SDS	Y	Y	Y
RC & TWEEN	-	-	-









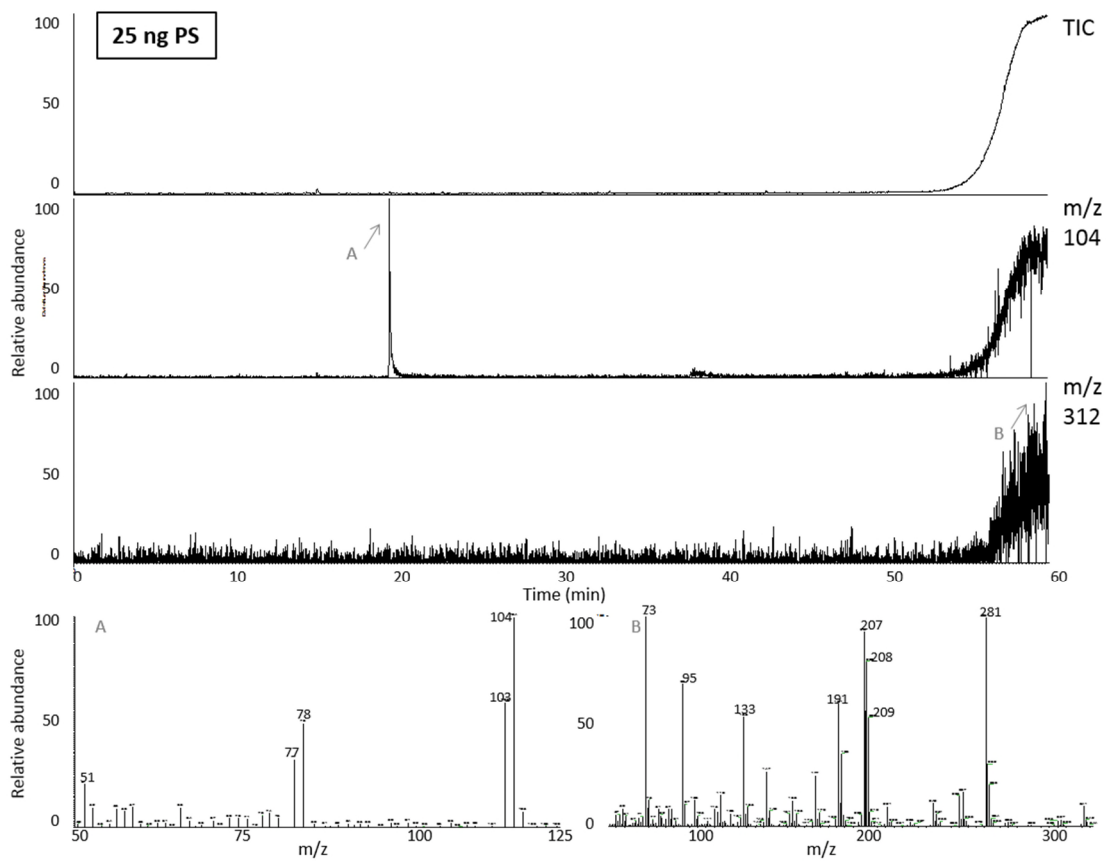


**Figure S3:** The pyrograms of a PS standard, and of PS (30  $\mu\text{g}$  to 25 ng) that was added to surface water samples after analysis with Pyrolysis GC-MS. Each showing the total ion current (TIC), the chromatogram of selected masses (styrene m/z 104; tri-styrene m/z 312) and the mass spectra of selected peaks (A, B).

## References

1. H. R. Veenendaal and A. J. Brouwer-Hanzens, *A method for the concentration of microbes in large volumes of water*, 2007.